



CIDE domains form functionally important higher-order assemblies for DNA fragmentation

Jae Young Choi^{a,1}, Qi Qiao^{b,c,1}, Se-Hoon Hong^d, Chang Min Kim^a, Jae-Hee Jeong^e, Yeon-Gil Kim^e, Yong-Keun Jung^d, Hao Wu^{b,c,2}, and Hyun Ho Park^{a,2}

^aSchool of Chemistry and Biochemistry and Graduate School of Biochemistry, Yeungnam University, Gyeongsan 712-749, South Korea; ^bDepartment of Biological Chemistry and Molecular Pharmacology, Harvard Medical School, Boston, MA 02115; ^cProgram in Cellular and Molecular Medicine, Boston Children's Hospital, Boston, MA 02115; ^dSchool of Biological Science, Seoul National University, Seoul 151-747, South Korea; and ^ePohang Accelerator Laboratory, Pohang University of Science and Technology, Pohang 790-784, South Korea

Contributed by Hao Wu, June 2, 2017 (sent for review April 10, 2017; reviewed by Gabriel Núñez, Xiaodong Wang, and T. Sam Xiao)

Cell death-inducing DFF45-like effector (CIDE) domains, initially identified in apoptotic nucleases, form a family with diverse functions ranging from cell death to lipid homeostasis. Here we show that the CIDE domains of *Drosophila* and human apoptotic nucleases Drep2, Drep4, and DFF40 all form head-to-tail helical filaments. Opposing positively and negatively charged interfaces mediate the helical structures, and mutations on these surfaces abolish nuclease activation for apoptotic DNA fragmentation. Conserved filamentous structures are observed in CIDE family members involved in lipid homeostasis, and mutations on the charged interfaces compromise lipid droplet fusion, suggesting that CIDE domains represent a scaffold for higher-order assembly in DNA fragmentation and other biological processes such as lipid homeostasis.

CIDE family | higher-order structure | DNA fragmentation | apoptosis | lipid homeostasis

A hallmark of apoptosis is the fragmentation of cellular genomic DNA into a ladder pattern composed of multiples of 180- to 200-bp pieces, which correspond to the DNA length in a nucleosome. Two decades ago, the enzyme responsible for regulated DNA fragmentation was identified from human HeLa cells as a heterodimeric complex of the nuclease DNA fragmentation factor (DFF) of 40 kDa (DFF40), and the inhibitor of 45 kDa (DFF45) (1). Independently, a heterodimeric complex of caspase-activated DNase (CAD) and its inhibitor (ICAD) was identified from mouse lymphoma cells (2, 3). DFF45 and ICAD chaperone the folding of DFF40 and CAD, respectively, and also trap them in inactive states through complex formation. On induction of apoptosis, DFF45 and ICAD are cleaved by activated caspases to release DFF40 and CAD for nuclear translocation and digestion of genomic DNA through large-scale chromatin fragmentation and internucleosomal DNA cleavage (1, 4).

DNA fragmentation is the basis for the classical apoptotic TUNEL assay that detects DNA double-strand breaks (5). Because apoptotic cells display “eat-me” signals and are phagocytosed, DNA fragmentation has been proposed as a mechanism for avoiding the transformation of recipient cells by the activated oncogenes or viral genes and reduce the autoimmune response from the strong autoantigenic DNA (6). Clinically, sperm DNA fragmentation is used as a correlative to male infertility (7), and circulating fragmented cell-free DNA is detected as a disease biomarker (8).

Human DFF40 and DFF45 and mouse CAD and ICAD contain a conserved N-terminal region known as the cell death-inducing DFF45-like effector (CIDE) domain (9) (Fig. S14). In *Drosophila*, four DFF-related proteins (Drep1–4) are critical for apoptotic DNA fragmentation (10–12) (Fig. S14), and Drep2 also acts as a unique synaptic protein important in learning and behavioral adaptation (13). Biochemical characterization of CIDE–CIDE interactions from Drep1 to Drep4 has revealed that the Drep2 and Drep4 nucleases interact with and are inhibited by Drep1 and Drep3 (14–16). In addition to DNA fragmentation, the CIDE domain-containing proteins CIDEA, CIDEB, and FSP27 (also known as CIDEc) play important roles in lipid homeostasis (17)

(Fig. S14), and their disruption can result in obesity, diabetes, liver steatosis, and cardiovascular diseases. CIDEA, CIDEB, and FSP27 are known to localize at lipid droplet contact sites, promoting lipid transfer and lipid droplet fusion in adipocytes and hepatocytes (17, 18).

CIDE domains possess an α/β roll structure with two α -helices and five β -strands as determined by NMR spectroscopy (19). NMR structures of CIDE domain complexes of DFF40–DFF45 and CAD–ICAD exhibit asymmetric heterodimers with charge complementarity (20, 21), and the crystal structure of the CIDE domain of FSP27 shows the molecular basis of homodimerization (22, 23). In the present study, examination of the crystal structures of Drep2 and Drep4 unexpectedly revealed that some CIDE domains also form higher-order assemblies through open-ended helical oligomerization to execute their diverse biological functions. This study establishes a domain scaffold for helical oligomerization from DNA fragmentation to lipid droplet metabolism.

Results

Crystal Structures of Drep2 and Drep4 Reveal CIDE Domain Helical Oligomerization. In an effort to shed light on the mechanism of DNA fragmentation, we determined the crystal structures of the

Significance

Cell death-inducing DFF45-like effector (CIDE) domains, initially identified in apoptotic nucleases, form a highly conserved family with diverse functions ranging from cell death to lipid homeostasis and synaptic regulation. Through structural determination of two CIDE family proteins, Drep2 and Drep4, we found that CIDE domains can form helical oligomers. Our results reveal that such higher-order structures not only are conserved in the CIDE family, but also are critically important for both DNA fragmentation and lipid droplet fusion. Therefore, our findings identify the CIDE domain as a scaffolding component for higher-order structure assembly. Our results expand the importance of higher-order structures from the established field of immune signaling to broader biological functions.

Author contributions: J.Y.C., Q.Q., S.-H.H., C.M.K., H.W., and H.H.P. designed research; J.Y.C., Q.Q., S.-H.H., C.M.K., J.-H.J., Y.-G.K., Y.-K.J., and H.H.P. performed research; J.Y.C., Q.Q., and H.H.P. contributed new reagents/analytic tools; J.Y.C., Q.Q., S.-H.H., C.M.K., J.-H.J., Y.-G.K., Y.-K.J., H.W., and H.H.P. analyzed data; and Q.Q., H.W., and H.H.P. wrote the paper.

Reviewers: G.N., University of Michigan; X.W., National Institute of Biological Sciences, Beijing; and T.S.X., Case Western Reserve University.

The authors declare no conflict of interest.

Data deposition: The atomic coordinates and structure factors have been deposited in the Protein Data Bank, www.pdb.org [PDB ID codes 4D2K (Drep2 CIDE domain), 5XPD (Drep4 CIDE domain P1 form), and 5XPC (Drep4 CIDE domain P212121 form)].

¹J.Y.C. and Q.Q. contributed equally to this work.

²To whom correspondence may be addressed. Email: wu@crystal.harvard.edu or hyunho@ynu.ac.kr.

This article contains supporting information online at www.pnas.org/lookup/suppl/doi:10.1073/pnas.1705949114/-DCSupplemental.

CIDE domains of the Drep4 nuclease in the crystal forms of P1 and P2₁2₁ at 3.0 and 1.9 Å resolution, respectively, and of the Drep2 nuclease in the P2₁2₁ space group at 2.3 Å resolution (Table S1). Surprisingly, these structures invariably revealed helical assemblies that have not been reported previously for any CIDE domains despite extensive structural study (19–22). In fact, it is usually impossible to crystallize a helical structure unless the helical periodicity happens to be an integer, as is the case here. The 10 molecules per crystallographic asymmetric unit in the P1 Drep4 structure form one turn of a helical assembly (Fig. 1A). In the crystal lattice, the helical structure is continuous and stacks along the *a*-axis of the unit cell with a 56.5 Å rise/turn and ~105 Å diameter. This arrangement is conserved in the P2₁2₁ Drep4 structure with five molecules in each crystallographic asymmetric unit (Fig. 1B). The Drep2 crystal contains four molecules in the crystallographic asymmetric unit, arranged into a helical assembly in the crystal with eight subunits per turn with a rise of 50.3 Å and diameter of ~90 Å (Fig. 1C). If one of the subunits in a Drep4 spiral is aligned with a subunit in a Drep2 spiral, then the neighboring subunits are related by a ~19° rotation (Fig. 1D).

To corroborate the crystal structures, we turned to electron microscopy (EM). Both Drep2 and Drep4 eluted from a Superdex

200 gel filtration column close to the void volume in a physiological salt condition of 150 mM NaCl and migrated at smaller sizes with increasing salt concentration (Fig. S1B). EM of negatively stained samples showed that Drep4 and Drep2 both formed rings and filaments, with comparable diameters in each of the crystals (Fig. 1E).

The Observed Interface is Responsible for Drep Helical Oligomerization.

The Drep2 and Drep4 helical oligomers are formed by repetitive head-to-tail polymerization between highly charged interfaces (Fig. 2A and B). In Drep4, residues D91, E94, D97, E99, and D116 form the highly negatively charged patch in opposition of residues K51, R59, K60, and K74 on the positively charged patch (Fig. 2B and C). These residues are largely conserved in Drep2 (Fig. S24). In both Drep2 and Drep4, this interface buries an ~500 Å² accessible surface area per subunit. To confirm the interface in Drep4, we generated mutations K51E, K74E, D91K, D97K, and E99K to disrupt the interfaces. Although the wild-type (WT) Drep4 CIDE domain eluted predominantly in an oligomer position in size exclusion chromatography, all five mutants showed reduced oligomerization (Fig. 2D). In addition, negative-staining

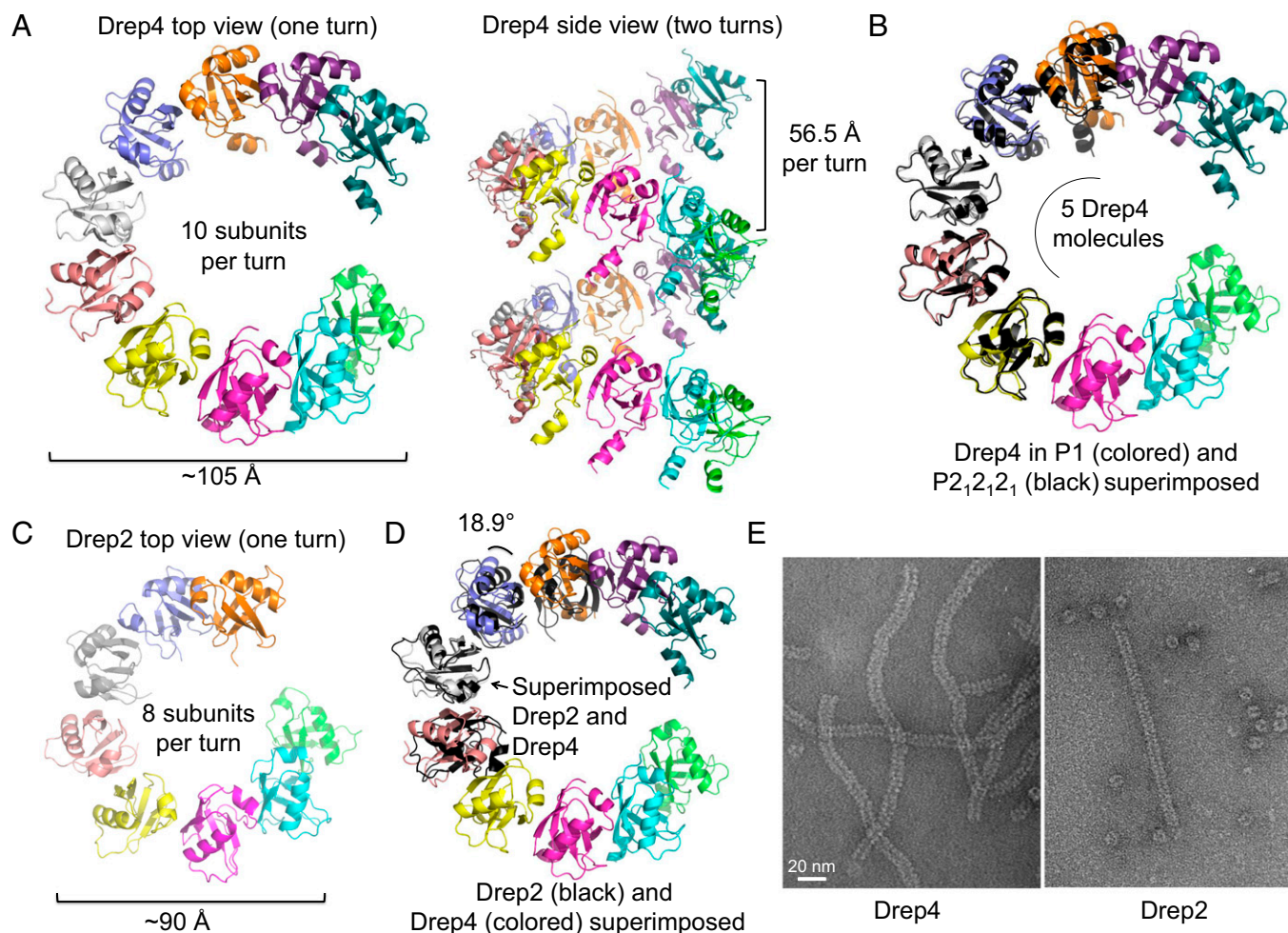


Fig. 1. Helical assemblies of Drep4 and Drep2 CIDE domains in crystals and in solution. (A) The helical assembly of Drep4 CIDE domain in an asymmetric unit of the P1 forms a crystal structure, with 10 subunits per turn. Each subunit is shown in a different color. (B) Structural alignment of the five Drep4 molecules in the P2₁2₁ crystal form (in black) with the 10 Drep4 molecules in the P1 crystal form (colored), showing a conserved helical arrangement. (C) Helical assembly of the Drep2 CIDE domain crystal structure with eight subunits per turn. (D) Structural alignment of the four molecules in the asymmetric unit of the Drep2 crystal with one turn of the Drep4 helix. The subunit used in the alignment is indicated. A Drep2 molecule adjacent to the aligned subunit needs to rotate by 18.9° to superimpose with the corresponding Drep4 molecule. (E) EM images of negatively stained Drep4 and Drep2 CIDE domains, showing rings and filaments.

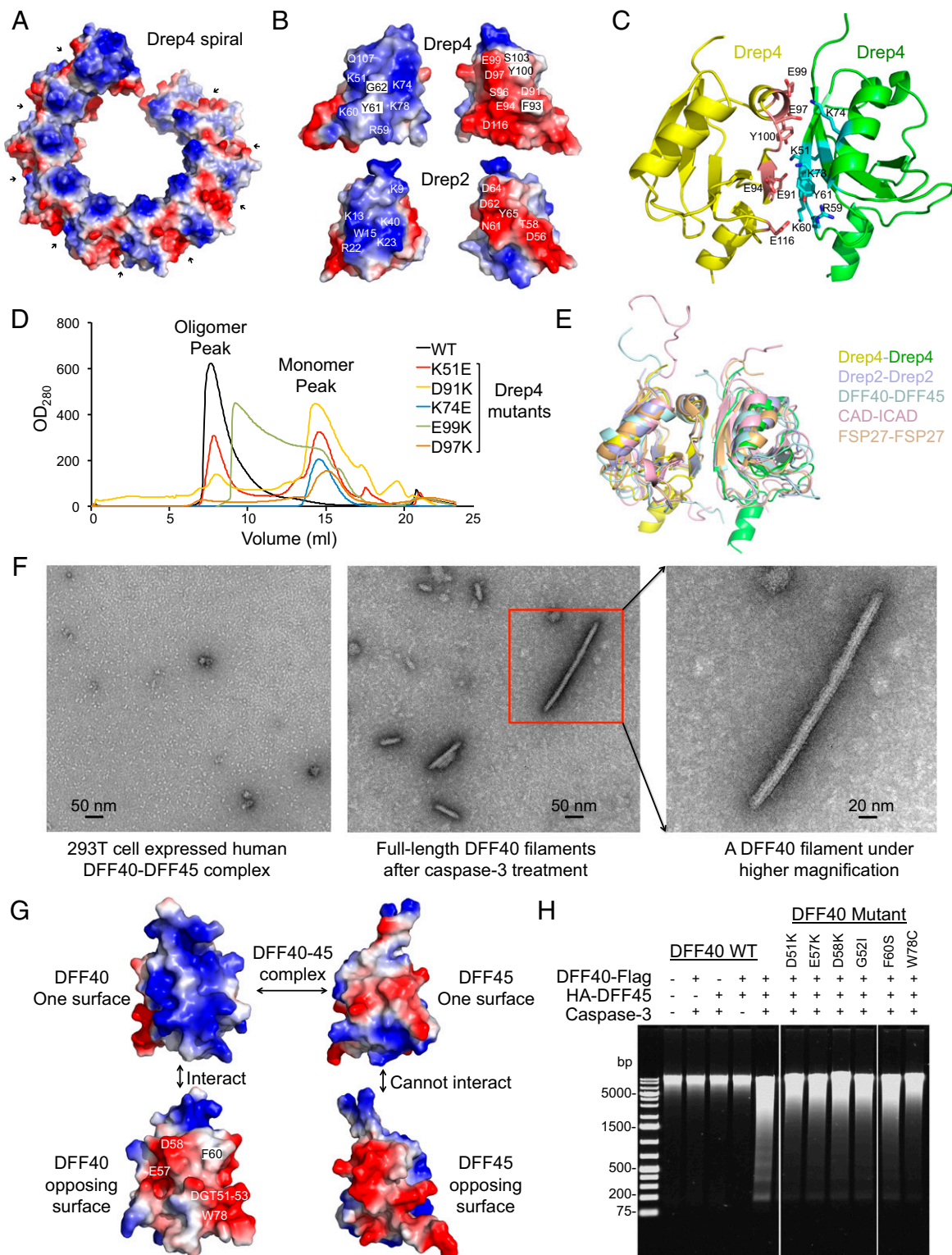


Fig. 2. Importance of CIDE domain oligomerization in DNA fragmentation. (A) Surface view of one turn of the Drep4 spiral with displayed electrostatics. (B) Striking charge complementarity at the interacting surfaces of Drep4 and Drep2 CIDE domains. (C) Residues at the Drep4 CIDE domain interface, with one subunit in yellow and the other subunit in green. The interfacial residues are colored, with oxygen atoms in red, nitrogen atoms in blue, and carbon atoms in pink and cyan. (D) Interfacial charge reversal mutations disrupt Drep4 CIDE domain oligomerization. (E) Structural alignment of a pair of Drep4 CIDE domains with those of a Drep2-Drep2 pair, the DFF40-DFF45 complex, the CAD-ICAD complex, and the FSP27 homodimer. (F) EM images showing the full-length DFF40-DFF45 complex before (Left) and after (Middle and Right) caspase-3 treatment. DFF40 released from DFF45 upon caspase-3 treatment shows filamentous structures. (G) Surface charge distributions of DFF40 and DFF45 CIDE domains, supporting DFF40, but not DFF45, homooligomerization. (H) In vitro DNA fragmentation assay. DFF40 CIDE domain oligomerization-deficient mutations significantly impaired nuclease activity.

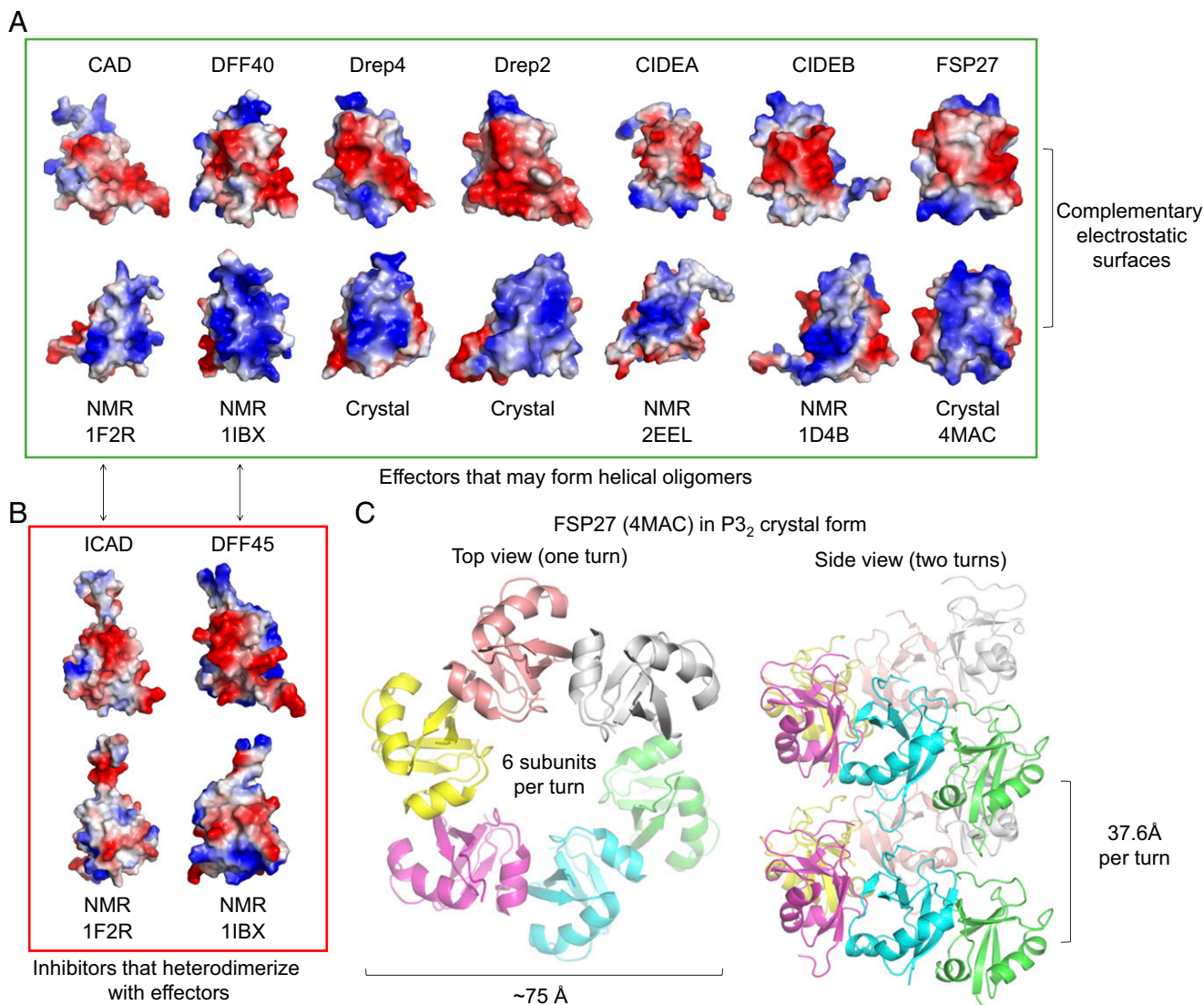


Fig. 3. Conserved helical oligomerization in the CIDE domain family. (A) The surface charge complementarity of CIDE family effector proteins supports homooligomerization. (B) The surface charge distribution of ICAD and DFF45, which are CIDE family inhibitor proteins, does not support homooligomerization. ICAD and DFF45 heterodimerize with CAD and DFF40, respectively. (C) Helical assembly of the FSP27 CIDE domain crystal structures with six subunits per turn (PDB ID code 4MAC).

EM revealed a lack of filament assembly by the five mutants (Fig. S2B), confirming compromised helical polymerization.

The DFF40 Nuclease Requires Helical Polymerization for DNA Fragmentation. We found that each Drep4–Drep4 and Drep2–Drep2 interface in the helical filament is very similar to the interfaces observed in the heterodimeric human DFF40–DFF45 and mouse CAD–ICAD CIDE domain complexes (20, 21) and in the homodimeric FSP27 complex (22, 23) (Fig. 2E). Like Drep2 and Drep4, the interaction between DFF40 and DFF45 involves a small hydrophobic cluster surrounded by salt bridges that include the conserved DGT motif (D51–T53 of DFF40) (20) (Fig. S24). Because earlier biochemical studies suggested that the DFF40 CIDE domain is oligomeric in the absence of DFF45 (20, 21), we wondered whether DFF40 also forms helical structures as Drep2 and Drep4. We coexpressed full-length WT Flag-tagged DFF40 (DFF40-Flag) with HA-tagged DFF45 (HA-DFF45), and immunopurified the complex using anti-Flag affinity gel (Fig. S2C and D). By adding recombinant active caspase-3 to the DFF40–DFF45 complex, we activated DFF40 by releasing the inhibition of

DFF45. Strikingly, EM revealed abundant filamentous structures only after caspase-3 treatment (Fig. 2F), indicating that DFF40 indeed forms helical higher-order structures on activation. These filaments are much wider, ~15 nm in diameter, consistent with a core of the CIDE domain flanked by the nuclease domain of DFF40.

Inspection of the surface charges of DFF40 CIDE domain revealed complementarity between the two opposing surfaces (Fig. 2G, Left), in contrast to the lack of complementarity for DFF45 (Fig. 2G, Right), further supporting the idea that the CIDE domain of DFF40 forms helical structures by head-to-tail polymerization. We reasoned that because the largely negatively charged surface of DFF40 is away from the DFF45-interacting surface, mutations on this surface might not affect the interaction with DFF45 but might only affect the oligomerization and possibly the nuclease activity of DFF40.

To test this hypothesis, we mutated E57, D58, and the conserved DGT motif, as well as the large hydrophobic residues F60 and W81, on the acidic surface of DFF40 (Fig. 2G, Bottom Left). We left the basic surface of DFF40 intact to preserve its interaction with DFF45.

Compared with WT DFF40, all mutants abolished filament assembly after caspase-3 treatment (Fig. S2E). Consistently, the DFF assay showed that only the coexpressed WT DFF40-DFF45 complex treated by caspase-3 exhibited robust DNA fragmentation activity (Fig. 2H). All six oligomerization-deficient DFF40 mutants maintained the interactions with DFF45 (Fig. S2D), but showed severely impaired DNA cleavage activity (Fig. 2H).

Helical Oligomerization and Functions of Other CIDE Domain Proteins. The surface features of the Drep2, Drep4, and DFF40 nucleases and the DFF45 inhibitor suggest that effectors in the DNA fragmentation pathway (Drep2, Drep4, and DFF40) exhibit self-complementary positive and negative surfaces to allow for homo-oligomerization by helical symmetry, whereas the inhibitor (DFF45) does not have opposing complementary surfaces and can heterodimerize only with the effector. To further investigate this observation, we analyzed the surface electrostatics of all CIDE family members with known structures and grouped them into those with self-complementary surfaces and those without these surfaces (Fig. 3A and B). As expected, we found that ICAD has similar non-complementary surfaces as DFF45, and thus can only associate with CAD to inhibit CAD but cannot self-associate (Fig. 3B). Besides the nucleases, CIDEA, CIDEB, and FSP27 also display self-complementary electrostatic surfaces, suggesting that these proteins also may form higher-order structures to promote lipid droplet exchange and fusion (17).

Previous studies have noted FSP27 homodimers in their crystal structures (22, 23). We wondered if these homodimers further oligomerize into helical structures in the crystal lattices. Indeed, in both independent crystal forms P₃₂ and P₆₅, FSP27 packs into similar helical oligomers with six subunits per turn and a diameter of ~75 Å (Fig. 3C and Fig. S34). The rise per turn is 37.6 Å in the P₃₂ space group (Fig. 3C) and 45.0 Å in the P₆₅ space group (Fig. S34), suggesting some degree of plasticity in the subunit packing. We examined whether FSP27 forms filaments in solution using EM, and found that the purified CIDE domain of FSP27 displays a filamentous morphology similar to Drep2 and Drep4 with a diameter of ~8 nm (Fig. S3B), which is consistent with the crystal structures and confirms the helical assembly of FSP27. The importance of FSP27 oligomerization is supported by previous mutations on the positively charged surface (R46E and R55E) and the

negatively charged surface (E87Q/D88N) that abolishes FSP27-mediated lipid droplet growth (23) (Fig. S3C).

Discussion

Oligomerization of DFF40 May Promote Nuclease Domain Dimerization and Activation. Why does the lack of oligomerization compromise the DNA fragmentation activity of apoptotic nucleases? As demonstrated by the crystal structure, the nuclease domain of CAD can only function as a dimer, yet its dimer interface is loosely packed with poorly defined electron densities (24). We suggest that the intrinsically weak nuclease dimers require that the nuclease domains be brought into proximity by the CIDE domains. This idea is supported by the earlier in vitro observation that on treatment of the DFF40/DFF45 complex by caspase-3, only the oligomeric fraction of DFF40 was associated with catalytic activity, whereas the monomeric fraction was inactive (25). Although the size distribution of DFF40 helical oligomers may differ in cells, the mechanism of oligomerization-driven activation remains the same. Thus, release from their inhibitors is not sufficient for activation of apoptotic nucleases. Instead, helical oligomerization of apoptotic nucleases is a missing step in their activation, which promotes nuclease dimerization for DNA fragmentation.

Therefore, caspase-mediated activation of apoptotic nucleases may proceed in several steps (Fig. 4). In a basal state, a nuclease binds its inhibitor using both the CIDE and inhibitor/chaperone domains (Fig. S14) to form an inactive heterodimer. On induction of apoptosis, the caspase cascade cleaves the inhibitor, releasing the nuclease for nuclear translocation. The monomeric nuclease then oligomerizes via its CIDE domain, which efficiently brings the nuclease domain into proximity for dimerization and thus catalytic activation, in a manner analogous to many caspase-activating complexes (26, 27). The dimeric nuclease domain exhibits the shape of molecular scissors, with the distance between the blades compatible with a dsDNA strand (24). The deep active-site crevice may distinguish internucleosomal DNA from nucleosomal DNA to generate apoptotic DNA ladders.

A Scaffold for Helical Oligomerization and Function. In recent years, higher-order assemblies have been identified as mechanisms of signaling in cell death and immunity (27, 28). In particular, the death domain (DD) fold superfamily members, including DD,

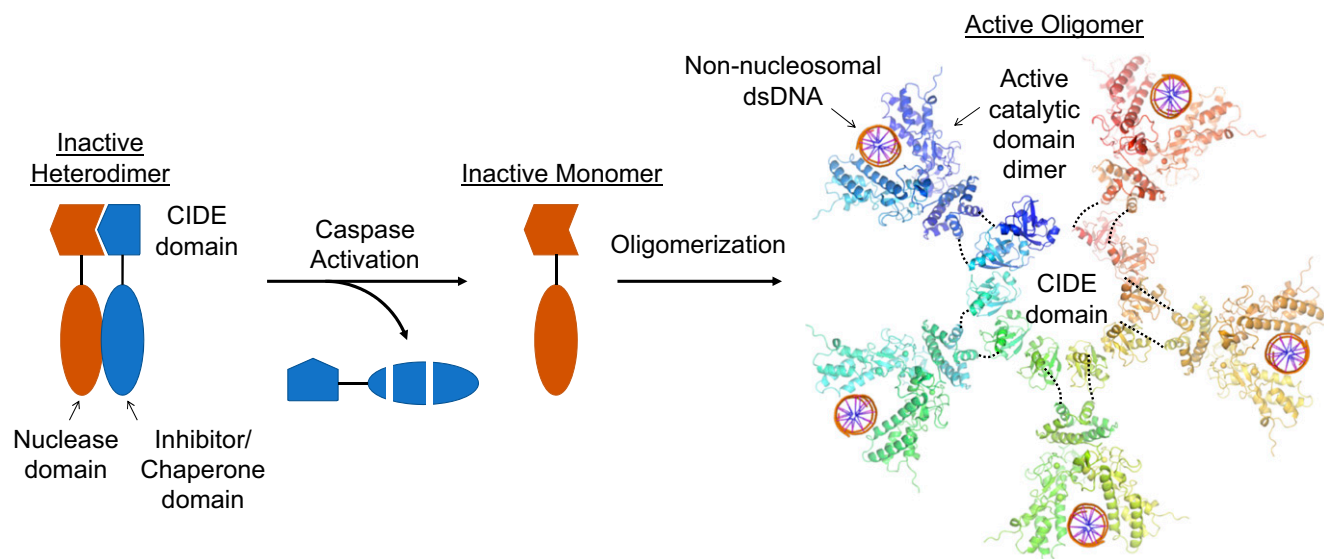


Fig. 4. A model of CIDE domain oligomerization in activation of apoptotic nucleases in DNA fragmentation. The nuclease domain structure of mouse CAD (PDB ID code 1V0D) was used (24).

CARD, PYD, and DED, ubiquitously form helical assemblies to mediate signal transduction, signal amplification, and proximity-induced enzyme activation. Our present study demonstrates that the CIDE domain family proteins form kinds of higher-order structures, which provide insight into CIDE domain-mediated processes ranging from DNA fragmentation to lipid droplet exchange and fusion. We do not yet know how higher-order structures facilitate lipid droplet homeostasis; however, in analogy to apoptotic nucleases and DD-mediated caspase and kinase activation, we suspect that the increased local concentration by oligomerization also may promote the lipid-binding activity of CIDEA, CIDEB, and FSP27.

Unlike the more stable cooperatively formed DD filaments, the head-to-tail oligomerization observed for CIDE domains may be more dynamic in assembly and disassembly and is reminiscent of the head-to-tail oligomerization by PB1, DIX, and SAM domains (28). In general, open-ended oligomers pose challenges to structural biology; they are often ignored because of their apparent size heterogeneity, and their structural mechanisms of assembly may be more difficult to elucidate. When the oligomerization leads to ordered assemblies such as the CIDE domain filaments, structure determination may be achieved by cryo-EM and sometimes by crystallography. When the oligomerization is less ordered and more dynamic, investigation with multiple approaches may be required to tease out the mechanisms. Perhaps because of these challenges, it is likely that many more higher-order structures exist

in diverse biological functions that have escaped our attention so far.

Materials and Methods

Sequence Alignment. The amino acid sequence of CIDEs was analyzed using ClustalW2 (www.ebi.ac.uk/Tools/msa/clustalw2/).

Protein Purification and Structure Determination. The expression and purification of Drep2 and FSP27 have been described in detail elsewhere (22, 29). Drep4 CIDE was produced using a previously established method (30). Further details are provided in *SI Materials and Methods*.

In Vitro DFF Assay. The DFF assay was performed as described previously (1). Details of the experiments are provided in *SI Materials and Methods*.

Electron Microscopy. The samples were imaged using a Tecnai G² Spirit BioTWIN Transmission Electron Microscope (TEM) and recorded with an AMT 2k CCD camera at the Harvard Medical School Electron Microscopy Facility. Details are provided in *SI Materials and Methods*.

ACKNOWLEDGMENTS. We thank Dr. Gabriel Núñez for advice regarding the DNA fragmentation assay setup. This study was supported by the Basic Science Research Program through the National Research Foundation of the Ministry of Education, Science and Technology (Grant NRF-2015R1D1A1A01057591, to H.H.P.), the Korea Healthcare Technology R&D Project of the Ministry of Health and Welfare, Republic of Korea (Grant HI13C1449, to H.H.P.), and the National Institutes of Health (Grant 1DP1 HD087988, to H.W.).

- Liu X, Zou H, Slaughter C, Wang X (1997) DFF, a heterodimeric protein that functions downstream of caspase-3 to trigger DNA fragmentation during apoptosis. *Cell* 89:175–184.
- Enari M, et al. (1998) A caspase-activated DNase that degrades DNA during apoptosis, and its inhibitor ICAD. *Nature* 391:43–50.
- Sakahira H, Enari M, Nagata S (1998) Cleavage of CAD inhibitor in CAD activation and DNA degradation during apoptosis. *Nature* 391:96–99.
- Sakahira H, Enari M, Ohsawa Y, Uchiyama Y, Nagata S (1999) Apoptotic nuclear morphological change without DNA fragmentation. *Curr Biol* 9:543–546.
- Gavrieli Y, Sherman Y, Ben-Sasson SA (1992) Identification of programmed cell death in situ via specific labeling of nuclear DNA fragmentation. *J Cell Biol* 119:493–501.
- Nagata S (2000) Apoptotic DNA fragmentation. *Exp Cell Res* 256:12–18.
- Agarwal A, et al. (2016) Clinical utility of sperm DNA fragmentation testing: Practice recommendations based on clinical scenarios. *Transl Androl Urol* 5:935–950.
- Tamkovich SN, Kirushina NA, Voytsitskiy VE, Tkachuk VA, Laktionov PP (2016) Features of circulating DNA fragmentation in blood of healthy females and breast cancer patients. *Adv Exp Med Biol* 924:47–51.
- Inohara N, Koseki T, Chen S, Wu X, Núñez G (1998) CIDE, a novel family of cell death activators with homology to the 45-kDa subunit of the DNA fragmentation factor. *EMBO J* 17:2526–2533.
- Mukae N, et al. (2000) Identification and developmental expression of inhibitor of caspase-activated DNase (ICAD) in *Drosophila melanogaster*. *J Biol Chem* 275:21402–21408.
- Inohara N, Núñez G (1999) Genes with homology to DFF/CIDEs found in *Drosophila melanogaster*. *Cell Death Differ* 6:823–824.
- Yokoyama H, et al. (2000) A novel activation mechanism of caspase-activated DNase from *Drosophila melanogaster*. *J Biol Chem* 275:12978–12986.
- Andlauer TF, et al. (2014) Drep-2 is a novel synaptic protein important for learning and memory. *eLife* 3:e03895.
- Lee SM, Park HH (2014) In vitro analysis of the complete CIDE domain interactions of the Drep system in fly. *Apoptosis* 19:428–435.
- Park OK, Park HH (2012) Dual apoptotic DNA fragmentation system in the fly: Drep2 is a novel nuclease of which activity is inhibited by Drep3. *FEBS Lett* 586:3085–3089.
- Park OK, Park HH (2013) A putative role of Drep1 in apoptotic DNA fragmentation system in fly is mediated by direct interaction with Drep2 and Drep4. *Apoptosis* 18:385–392.
- Xu L, Zhou L, Li P (2012) CIDE proteins and lipid metabolism. *Arterioscler Thromb Vasc Biol* 32:1094–1098.
- Xu W, et al. (2016) Differential roles of cell death-inducing DNA fragmentation factor- α -like effector (CIDE) proteins in promoting lipid droplet fusion and growth in subpopulations of hepatocytes. *J Biol Chem* 291:4282–4293.
- Lugovskoy AA, et al. (1999) Solution structure of the CIDE-N domain of CIDE-B and a model for CIDE-N/CIDE-N interactions in the DNA fragmentation pathway of apoptosis. *Cell* 99:747–755.
- Zhou P, Lugovskoy AA, McCarty JS, Li P, Wagner G (2001) Solution structure of DFF40 and DFF45 N-terminal domain complex and mutual chaperone activity of DFF40 and DFF45. *Proc Natl Acad Sci USA* 98:6051–6055.
- Otomo T, Sakahira H, Uegaki K, Nagata S, Yamazaki T (2000) Structure of the heterodimeric complex between CAD domains of CAD and ICAD. *Nat Struct Biol* 7:658–662.
- Lee SM, Jang TH, Park HH (2013) Molecular basis for homo-dimerization of the CIDE domain revealed by the crystal structure of the CIDE-N domain of FSP27. *Biochem Biophys Res Commun* 439:564–569.
- Sun Z, et al. (2013) Perilipin1 promotes unilocular lipid droplet formation through the activation of Fsp27 in adipocytes. *Nat Commun* 4:1594.
- Woo EJ, et al. (2004) Structural mechanism for inactivation and activation of CAD/DFF40 in the apoptotic pathway. *Mol Cell* 14:531–539.
- Liu X, Zou H, Widlak P, Garrard W, Wang X (1999) Activation of the apoptotic endonuclease DFF40 (caspase-activated DNase or nuclease): Oligomerization and direct interaction with histone H1. *J Biol Chem* 274:13836–13840.
- Salvesen GS, Dixit VM (1999) Caspase activation: The induced-proximity model. *Proc Natl Acad Sci USA* 96:10964–10967.
- Wu H (2013) Higher-order assemblies in a new paradigm of signal transduction. *Cell* 153:287–292.
- Wu H, Fuxreiter M (2016) The structure and dynamics of higher-order assemblies: Amyloids, signalosomes, and granules. *Cell* 165:1055–1066.
- Lee SM, Park HH (2014) Purification, crystallization and preliminary X-ray crystallographic studies of Drep2 CIDE domain. *Acta Crystallogr F Struct Biol Commun* 70:1414–1417.
- Walden H (2010) Selenium incorporation using recombinant techniques. *Acta Crystallogr D Biol Crystallogr* 66:352–357.
- Otwinowski Z, Minor W (1997) Processing of X-ray diffraction data collected in oscillation mode. *Methods Enzymol* 276:307–326.
- Adams PD, et al. (2010) PHENIX: A comprehensive Python-based system for macromolecular structure solution. *Acta Crystallogr D Biol Crystallogr* 66:213–221.
- Emsley P, Cowtan K (2004) Coot: Model-building tools for molecular graphics. *Acta Crystallogr D Biol Crystallogr* 60:2126–2132.
- Laskowski RA, MacArthur MW, Moss DS, Thornton JM (1993) PROCHECK: A program to check the stereochemical quality of protein structures. *J Appl Cryst* 26:283–291.